CHEMIJA. 2005. T. 16. Nr. 3-4. P. 15–20

Template-assisted fabrication of pure Se nanocrystals in controllable dimensions

Arûnas Jagminas[1*],

Indrë Gailiûtë[2],

Gediminas Niaura[1],

Raimondas Giraitis[1]

[1] *Institute of Chemistry, Goštauto 9, 01108 Vilnius, Lithuania*

[2] *Department of General and Inorganic Chemistry, Vilnius University, Naugarduko 24, 2734 Vilnius, Lithuania*

Selenium particles up to about 100 nm in height and diameter (¨) close to ¨ of alumina pores within [10; 70] nm range are fabricated by porous alumina alternating current (AC) electrolysis in the selenious acid solution route. The controllable dimensions of nanoparticles were achieved mainly by controlling the pore ¨ of alumina matrices and the temperature of the deposition bath. Off-resonance FT-Raman spectra excited at 1064 nm revealed that as-grown nanoscale particles are composed from the disordered nearly-free helical chains of amorphous a-Se containing some quantity of trigonal t-Se and Se_8 rings. FT-Raman, XRD and UV-vis spectra showed that after annealing in argon atmosphere at 438 K these nanoparticles exhibit a perfect *hcp* lattice of crystalline t-Se.

Key words: alumina matrix, selenium, nanoparticles, ac electrolysis, FT-Raman, XRD and UV-vis spectra, SEM

INTRODUCTION

The growing interest of scientists and technologists in fabricating and investigating the features of nanomaterials is related with their interesting and novel size- and composition-dependent properties in times overtaking the ones of the bulk. Notably, the properties of materials in the nanometer scale are dependent not only on the particle dimensions and the arrangement amongst them, but also on the manner in which they are organized. Owing to this, high-ordered oxide films fabricated by two-step [1, 2] or pre-textured [3, 4] anodizing of pure and smooth aluminium surface [5] in a solution of certain acid recently occupy a strategic position in materials science as the most versatile and promising templates for electrochemical and thermal synthesis of various nanoscale wires [6, 7] and tubes [8, 9] in controllable dimensions and spacing. However, to the best of our knowledge, the works related to the synthesis of selenium species within the pores of alumina matrices are scarce. On the other hand, nanoscale selenium particles due to their excellent photoelectrical performance, semiconductor properties and high biological activity have attracted recently steadily growing attention [10–12]. Most of these studies are deal with selenium species incorporated within the pores of zeolites by hydrothermal, vapour adsorption, or solution-phase methods where formation of helix Se chains containing additionally some quantity of Se_8, Se_6, or Se_3 rings [13–17] has been shown.

Here we, for the first time, report the electrochemical synthesis of pure trigonal t- selenium tablet-shaped nanocrystals in predicted dimensions by the one-step AC deposition process from an aqueous solution of selenious acid, followed by thermally induced re-crystallization in argon atmosphere.

EXPERIMENTAL

Flag-shaped specimens 15 × 15 × 0.125 mm, in dimensions cut from high purity aluminium foil (99.99% Al, Goodfellow Ltd.) were used in this study. After annealing at 773 K for 3 h the aluminium electrodes were cleaned and electropolished in a perchloric acid – ethanol bath at 17 V DC for 4 min according to conventional procedures [18]. Then the specimens were twice anodized in a vigorously stirred aqueous solution of 0.3 M oxalic acid at 290 K and 40 V DC for 3 h and 1 h, respectively [19]. After the first anodization, the strip-off process was carried out in a solution of 0.4 M phosphoric and 0.2 M chromic acids kept at 333 K [1, 2] for 20 h leaving behind an aluminium surface textured with a hexagonal scalloped pattern. The thickness of alumina barrier-layer was reduced by lowering the anodizing voltage at the end of second anodization stepwise [20] down to 15 V. The sequential pore widening process was conducted in a solution containing

*E-mail: jagmin@ktl.mii.lt

0.5 M phosphoric acid kept at 303 K for 5 to 40 min. Thus, high-ordered alumina matrices 7.0 μm thick, with an average pore diameter in the range from 22 to 70 nm and interpore distance of 108 νm, determined from the SEM images (Fig. 1A) were fabricated for further studies. For some experiments the porous alumina with a finer porous configuration (¨ of pores from 10 to 15 νm) 10 μm in thickness were grown in an aqueous solution of 1.2 M H_2SO_4 kept at 283 K (U_a = 10 V; 1 h).

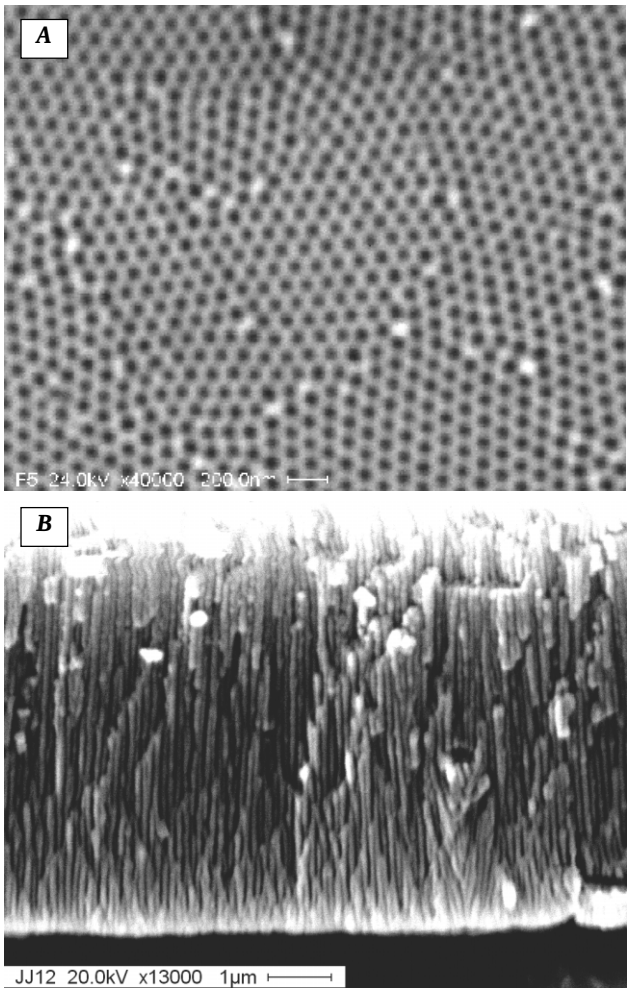

Fig. 1. SEM top- (***A***) and cross-sectional (***B***) view of alumina matrices grown by double anodization in a solution of 0.3 M $(COOH)_2$ at 290 K and 40 V for 3.0 and 1.0 h, respectively ($U_{a,fin}$ = 15 V), after subsequent etching of the matrix in 0.5 M H_3PO_4 at 303 K for 25 min (***A***) and AC deposition of selenium species (U_{pik} = 20 V; 313 K; 5 min) (***B***)

The alternating current (AC), 50 Hz in frequency, centering at 0 V, under constant peak voltage (U_{pik}) control equal to from 8 to 30 V was used for deposition of selenium species into alumina pores. Some experiments were conducted under AC current density control calculated for the apparent surface area of the electrode. An aqueous solution containing 0.2 M H_2SeO_3 and maintained at pH from 1.2 to 8.5 through the addition of boric, citric, or sulphuric acid, and / or triethanolamine (1:1) was employed. Two graphite rods were used as the auxiliary electrodes in the deposition bath thermostated within a 293–333 K range. All solutions were made up using triply distilled water, highest pure acids, and analytical grade salts (Aldrich).

A programmable furnace was used for annealing the alumina samples placed into a glass tube under conditions of continuous flow of purified argon gas.

UV-vis spectra of alumina/Se matrices detached from the surface were recorded using a Perkin Elmer Lambda 35 spectrometer.

The alumina matrices intended for XRD and UV-vis investigations were separated from the metal surface by dissolving aluminium in a solution of 10% HCl + 0.05 M $CuCl_2$ at 278 K. An X-ray D8 diffractometer (Bruker AXS, Germany) equipped with a Göbel mirror (primary beam monochromator) for CuK_α radiation was used for XRD analysis. In these measurements, continuous scan mode was used in the 22–55° 2Θ range with a scan rate of 1 degree per min.

Raman measurements were carried out with an FT-Raman spectrometer (Perkin Elmer, Model Spectrum GX) equipped with an InGaAs detector operating at room temperature [21]. The excitation was provided by an air-cooled diode-pumped Nd–YAG laser with an emission wavelength of 1064 nm. In order to reduce the photo- or thermo-effects, the sample was periodically moved with respect to the laser beam (at around 20 mm/s) [22].

The morphology of alumina and selenium species was investigated using a scanning electron microscope (Philips 30L) and a transmission electron microscope (TEM 100) under typical working conditions. For TEM observations of selenium nanoparticles, the alumina matrix was dissolved in a solution of 1.0 M phosphoric acid at 303 K for 48 h, leaving the species in the supernatant. Following centrifugation, these nanoscale particles were collected and thoroughly rinsed. Then for imaging they were dispersed in ethanol and replaced on a TEM carbon grid.

RESULTS AND DISCUSSION

Peculiarities of selenium deposition within the alumina template pores by alternating current electrolysis

It has been found here that the sallow colours of alumina matrices obtained usually by AC electrolysis in a solution of selenious acid kept at room temperature under conditions of this study are essentially identical independently of the AC voltage applied within the U_{pik} range of 8 to 30 V. It is worth noting that the colour tint of the electrode gained within a few minutes of AC electrolysis is close to that obtained during a prolonged process. Variations in the

solution acidity within (1.2–8.5) pH range by addition of sulphuric, citric, or boric acid, and / or triethanolamine did not show any noticeable changes in the colouration. In contrast, an increase in the bath temperature to 313–318 K leads to a much deeper colouration of alumina matrices in yellow-orange tints. Moreover, at elevated bath temperatures some dependence of the resulting alumina colours on the AC voltage value can be observed. Therefore, it is reasonable to suppose that selenium particles under the given bath temperature and AC voltage value incorporate within the alumina pores in the same quantity, dimensions, and composition. If so, one can expect that the result of alumina AC treatment in the solution of selenious acid, under conditions of constant bath temperature and AC voltage, must be dependent only on the real surface area at which the electrochemical reaction takes place.

This assumption was proved here by investigation of the matrix colours and the shapes of selenium particles upon the time of matrix pore widening in

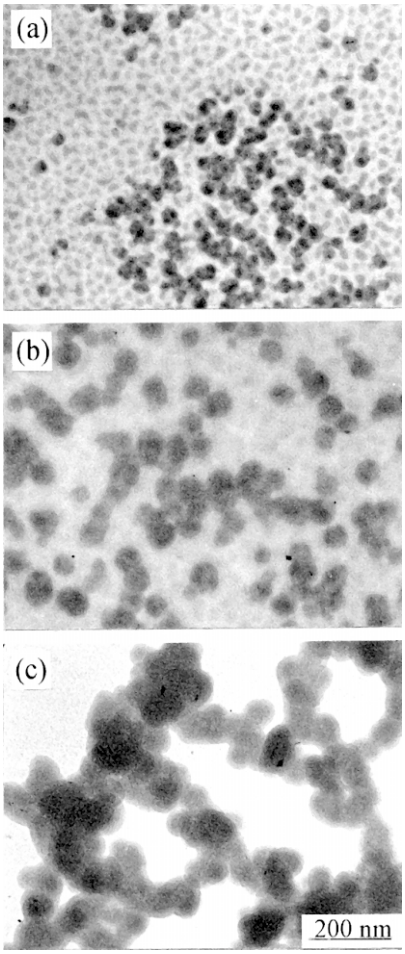

Fig. 2. TEM images of selenium particles liberated from the alumina on their pore diameter increased by etching the matrix in a solution of 0.5 M H_3PO_4 at 303 K for time (t_w): (*a*) 20, (*b*) 30, and (*c*) 35 min. The subsequent AC deposition of selenium was conducted in 0.2 M H_2SeO_3 + H_2SO_4 up to pH 1.7 at room temperature and $U_{pik} \le 15$ V ($j \le 5$ mA cm^{-2}) for 5 min

the etching solution (τ_w). The results obtained show that an increase in τ_w, and therefore in $\ddot{}_{pore}$ [23], leads to a much intensive colouring of the alumina in yellow-orange tints. Figure 2 illustrates the TEM images of selenium particles deposited within the alumina matrices of various porosity at room temperature and $j \le 5$ mA cm^{-2} until the same AC voltage value of $U_{pik} = 15$ V is achieved. Calculations from these images have showed that an increase in the τ_w leads to an increase in the diameter of deposited particles ($\ddot{}_{Se}$) in a manner similar to that of $\ddot{}_{pore}$ [23].

In addition, there is some part of selenium particles with dimensions much smaller than $\ddot{}_{pore}$ of the template used, implying the possibly of their crumbling during the separation process. The location of selenium particles within the cross-sections of alumina matrices and the thickness of the alumina layer filled with these particles was studied by scanning electron microscopy (SEM). This study has shown that the height of the alumina layer with the deposited selenium particles is located at the alumina / Al interface and depends mainly on the deposition bath temperature and within a [293–333] K range amounts from ~20 to ~100 nm (Fig. 1B). Preliminary results have shown that this is also valid for alumina grown in a sulphuric acid bath where oxide matrices with a finer structure ($\ddot{}_{pore}$ from 10 to 15 nm [24]) are fabricated. Therefore, it is reasonable to conclude that controllable synthesis of selenium tablet-shaped nanoparticles is possible by AC electrolysis of alumina matrices with the $\ddot{}_{pore}$ close to the required for $\ddot{}_{Se}$, at least within the range 10–70 nm.

An increase in the size of selenium species deposited into the alumina pores with an increase in $\ddot{}_{pore}$ was also verified from UV-vis spectra of alumina matrices detached from the aluminium surface. As is seen from Fig. 3, the spectra of alumina / Se films demonstrate plasmon resonance with a peak in a vicinity of 250 nm characteristic of selenium colloids. A red-shift of this peak, clearly seen with an increase in $\ddot{}_{pore}$ (curves 3–5), must be attributed to the increase in the size of Se particles as can be also expected from the deepness of the matrix colours.

Phase composition of as-grown selenium species

To gain further information about the crystal structure, molecular and phase composition of selenium particles confined within the alumina pores by AC electrolysis, XRD and Raman analysis have been performed. The resulting XRD spectra are shown in Fig. 4. Only one broad single peak was detected at a 2Θ angle of ~44.2° for the as-grown selenium nanoparticle array from the room temperature bath, showing thereby an extremely low crystallinity of the nanoscale product embedded within the alumina matrix by AC electrolysis. Notably, an increase in the

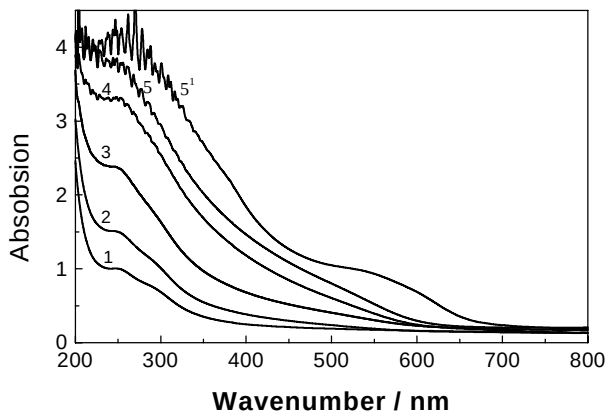

Fig. 3. UV-vis spectra of pure alumina matrix grown in 0.3 M $(COOH)_2$ solution for 2.0 h (*1*) and the same alumina matrices embedded with deposited selenium species on the alumina pores widening time: (*2*) 0; (*3*) 10; (*4*) 25; (*5*, *5'*) 35 min before (1–5) and after annealing in Ar atmosphere at 438 K for 1.0 h (*5'*). Se deposition conditions the same as in Fig. 2

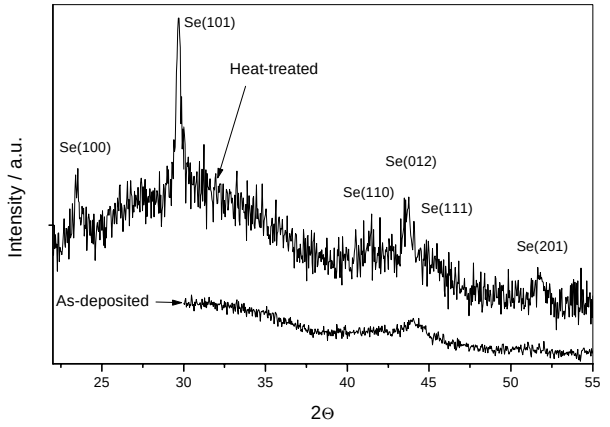

Fig. 4. XRD spectra of alumina matrices ($\ddot{}_{pore}$ ~50 nm) with deposited selenium nanoparticles (room temperature bath; U_{pik} 15 V; 5 min) before (*1*) and after (*2*) annealing them in pure Ar atmosphere at 438 K for 1 h

bath temperature up to 333 K and, as stated, in the height of selenium particles has little or no influence on their phase composition. However, it has been found herein that the crystalline structure of selenium particles changes drastically after annealing them in a pure argon atmosphere. Altogether, six diffraction peaks corresponding well to a hexagonal close-packed selenium (*hcp*) lattice (PDF No 65-1876) were observed within the 2Θ range 23–52°. This result differs from the structures of selenium nanowires synthesized by other methods where either trigonal [25], monoclinic [11], or *fcc* [26] nanocrystals have been fabricated.

The FT-Raman spectra of the alumina matrices with confined as-synthesized selenium nanoparticles are shown in Fig. 5. To avoid heating-induced broadening of the spectral bands [15] or photomelting of the confined selenium species [27], we have employed off-resonant excitation (1064 nm) of the Raman spectra. In this experiment, the density of laser power was reduced by using the moving sample setup [22]. As is seen from Fig. 5, the Se–Se stretching band at 251 cm^{-1} dominates the spectra. The position of this band does not depend on τ_w, while the integrated intensity increases sixfold when τ_w increases from 15 to 35 min. A more detailed analysis of the 251 cm^{-1} band (insert in Fig. 5) reveals a complex contour which was digitally decomposed into three Lorentzian–Gaussian components at 237, 251, and 261 cm^{-1}. The position of the intense 251 cm^{-1} component corresponds well to the frequency of the Se–Se symmetric stretching mode of the amorphous Se (a-Se) [27, 28]. a-Se can be considered as composed from disordered, nearly free helical chains with unequal signs and magnitudes of the dihedral angles [29]. The relatively narrow width (12.2 cm^{-1}), determined as the full width at half maximum (FWHM) of this component, indicates a rather regular structure of the a-Se chains in alumina pores. The lower frequency component at 237 cm^{-1} evidenced presence of trigonal t-Se [27, 30], while the relatively narrow (FWHM = 12.3 cm^{-1}) higher frequency 261 cm^{-1} peak was assigned to the Se–Se symmetric stretching vibration of Se_8 rings, based on the close frequency correspondence to the theoretically predicted value (259 cm^{-1}) for isolated S_8 rings [17]. Slightly higher stretching frequencies were detected

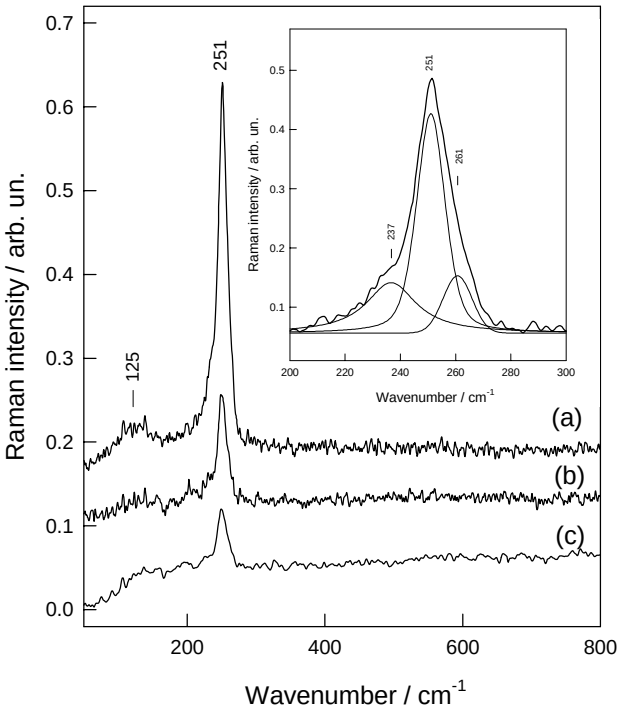

Fig. 5. FT-Raman spectra of alumina matrices with deposited selenium nanoparticles under conditions as in Fig. 2. Etching time of alumina matrices (τ_w): (*a*) 35, (*b*) 25, and (*c*) 15 min. Insert shows decomposition of the experimental curve (*b*) into the Lorentzian–Gaussain components (thinner lines). Excitation wavelength is 1064 nm. Resolution is 2 cm^{-1}. Spectra are vertically shifted for clarity

experimentally for S_8 rings confined in nanochannels of AlPO4-5 zeolite (268, 267 cm^{-1}) [15, 16] or mordenite (267 cm^{-1}) [29]. The structural deformations and interactions between the rings are probably responsible for the differences in frequencies. In addition to the stretching band, the Se–Se bond bending motion is represented by the broad feature at a vicinity close to 125 cm^{-1} (Fig. 5). Finally, it should be noted that no second order bands in the vicinity of 450–500 cm^{-1} were detected in the FT-Raman spectra of Se confined in alumina pores. Figure 6 shows the effect of selenium deposition temperature and subsequent annealing on the FT-Raman spectra. In agreement with XPS data, increasing the Se deposition temperature from 293 to 313 K does not affect the Raman spectrum.

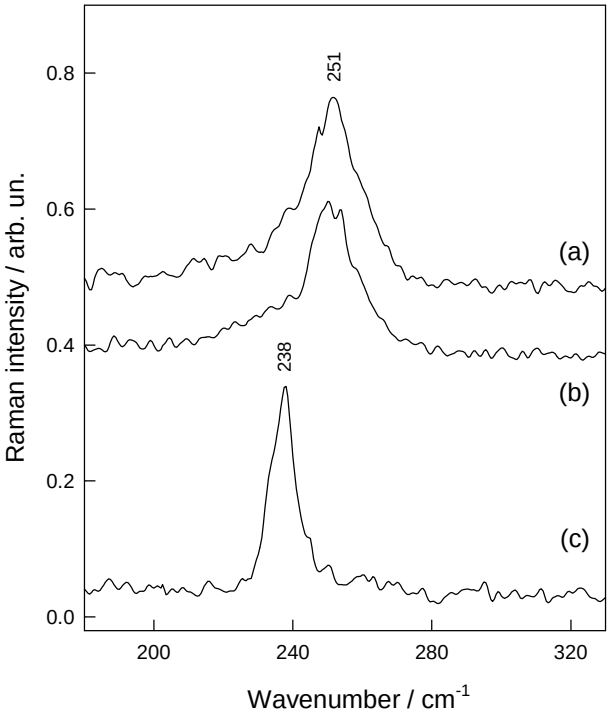

Fig. 6. FT-Raman spectra in the Se–Se bond stretching spectral region of alumina matrices with AC-deposited selenium nanoparticles before (*a, b*) and after (*c*) annealing at 438 K for 1.0 h. Se deposition bath temperature is 293 (*a*) and 313 K (*b, c*). Excitation wavelength is 1064 nm. Resolution is 2 cm^{-1}. Spectra are vertically shifted for clarity

Transformation of phase composition of nano-Se particles by thermal annealing

It has been found herein that drastic Raman spectral changes take place after annealing the alumina / Se samples at 438 K for 1 h (Fig. 6c) where the peak frequency shifts from 251 to 238 cm^{-1} and FWHM decreases from 16.1 to 8.6 cm^{-1}. These spectral changes indicate formation of crystalline well-ordered t-Se phase [27, 30].

The phase transformation of deposited selenium species by thermal treatment has been also verified from the UV-vis spectrum of annealed specimen presented in Fig. 4 (curve 5'), showing not only a red-shift plasmon resonance with a new peak at ~550 cm^{-1}, but also great changes in a broad spectral region starting from ~670 cm^{-1}, which can be attributed to the band gap changes of incubated nanomaterial.

It is worth noting that phase transformations of a-Se deposited into the crystalline phase of t-Se proceed only in the matrices detached from the aluminium substrate. Outwardly, annealing the Al / alumina / a-Se samples even in an argon atmosphere results in the disappearance of matrix colour. We suggest that this phenomenon could be related with the reaction of selenium atoms thermally diffused through the alumina barrier layer with aluminium. This suggestion was confirmed by SEM images of the sample cross-sections. As is clearly seen from Fig. 7, the nano-Se / alumina / Al interface changes drastically after annealing, showing a burst-like deface of the high-ordered morphology of the alumina matrix at the Al / oxide interface.

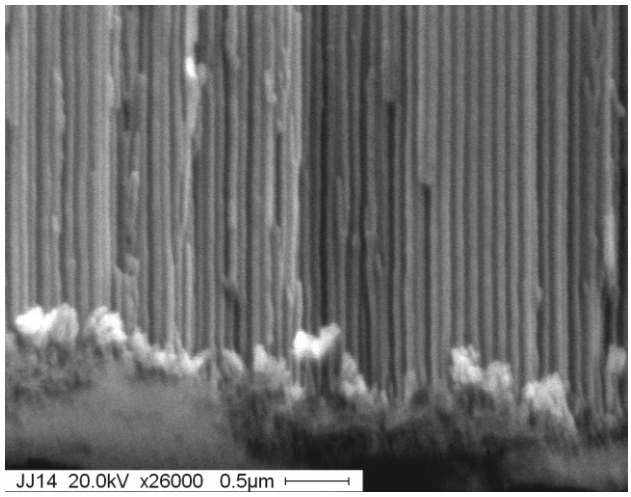

Fig. 7. Cross-sectional view of Al / alumina / a-Se contour grown and electrochemically filled with selenious species as in Fig. 1B after annealing at 438 K in argon atmosphere for 1.0 h

CONCLUSIONS

In conclusion, we have demonstrated the possibility to grow the nanoparticles of selenium up to ~100 nm in height and with a diameter close to the diameter of aluminium template pores (10–70) nm by one step AC deposition way. The FT-Raman spectra has shown that as-deposited Se nanoparticles consist predominantly of amorphous a-Se with small quantities of t-Se and S_8 rings. We have also demonstrated that after annealing at 438 K for 1 h in argon atmosphere, the amorphous Se nanoparticles in aluminium pores transform into the crystalline trigonal t-Se phase if the matrix is detached from the surface of aluminium. It seems that additional studies are required in order to establish the reasons for and

the kinetics of the retarded growth of selenium particles at the bottom of the alumina pores in a uniform height independently of the bath composition.

ACKNOWLEDGEMENT

Habil. Dr. R. Juðkënas, Dr. M. Kurtinaitienë and Dr. A. Jagminienë for experimental support with XRD, TEM and UV-vis studies. We also gratefully acknowledge the Department of Bioelectrochemistry and Biospectroscopy at the Institute of Biochemistry (Vilnius) for the possibility to use the FT-Raman spectrometer.

Received 24 October 2005
Accepted 05 December 2005

References

1. A. P. Li, F. Müller, A. Birner, K. Nielsch and U. Gösele, *J. Appl. Phys*. **84**, 6023 (1998).
2. A. P. Li, F. Müller, A. Birner, K. Nielsch and U. Gösele, *Adv. Mater*. **11**, 483 (1999).
3. H. Asoh, S. Ono, T. Hirose, M. Nakao and H. Masuda, *Electrochim. Acta* **48**, 3171 (2003).
4. H. Masuda, H. Yamada, M. Satoh, H. Asoh, M. Naka and T. Tamamura, *Appl. Phys. Lett*. **71**, 2770 (1997).
5. O. Jessensky, F. Müller and U. Gösele, *Appl. Phys. Lett*. **72**, 1173 (1998).
6. D. G. W. Goad and M. Moskovits, *J. Appl. Phys*. **49**, 2929 (1978).
7. A. Jagminas, *J. Appl. Electrochem*. **32**, 1201 (2002).
8. J. Li, M. Moskovits and T.L. Haslett, *Chem. Mater*. **10**, 1963 (1998).
9. J.S. Suh and J.S. Lee, *Appl. Phys. Lett*. **75**, 2047 (1999).
10. J. A. Johnson, M.-L. Saboungi, P. Thiyagarajan, R. Csencsits and D. Meiel, *J. Phys. Chem*. **B 103**, 59 (1999).
11. B. Gates, B. Mayers, B. Cattle and Y. Xia, *Adv. Funct. Mater*. **12/3**, 219 (2002).
12. X. Gao, J. Zhang and L. Zhang, *Adv. Mater*. **14/4**, 290 (2002).
13. J. B. Parise, J. E. Mac. Dougall, M. Herron, R. Farlee, A. W. Sleight, Y. Wang, T. Bein, K. Moller and L. M. Moroney, *Inorg. Chem*. **28**, 221 (1988).
14. Z. K. Tang, M. M. T. Loy, J. Chen and R. Xu, *Appl. Phys Lett*. **70**, 34 (1997).
15. V. V. Paborchii, A. V. Kolobov, J. Caro, V. V. Zhuravlev and K. Tanaka, *Chem. Phys. Lett*. **280**, 17 (1997).
16. I. L. Li, P. Launois and Z. K. Tang, *Appl. Surf. Sci*. **226**, 36 (2004).
17. A. Goldbach, L.E. Iton and M.-L. Saboungi, *Chem. Phys. Lett*. **281**, 69 (1997).
18. A. Jagminas, S. Lichusina, M. Kurtinaitienë and A. Selskis, *Appl. Surf. Sci*. **211**, 194 (2003).
19. Z. H. Yuan, H. Huang, L. Liu and S. S. Fan, *Chem. Phys. Lett*. **345**, 39 (2001).
20. R. C. Furneaux, W. R. Rigby and A. P. Davidson, *Nature* **337**, 147 (1989).
21. A. Jagminas, G. Niaura, A. Judþentienë and R. Juðkënas, *Appl. Surf. Sci*. **239**, 72 (2004).
22. G. Niaura, A. K. Gaigalas and V. L. Vilker, *J. Raman Spectrosc*. **28**, 1009 (1997).
23. D. Al-Mawlawi, Coombs and M. Moskovits, *J. Appl. Phys*. **70**, 979 (1991).
24. J. P. O'Sullivan and G. C. Wood, *Proc. R. Soc. London*, **A 317**, 511 (1970).
25. X. Gao, T. Gao and L. J. Zhang, *Mater. Chem*. **13**, 6 (2003).
26. X. Y. Zhang, Y. Cai, J. Y. Miao, K. Y. Ng, Y. F. Chan, X. X. Zhang and N. Wang, *J. Cryst. Growth* online (5 January 2005).
27. V. V. Poborchii, A. V. Kolobov and K. Tanaka, *Appl. Phys. Lett*. **74**, 215 (1999).
28. K. Nakamura and A. Ikawa, *J. Non-Cryst. Solids*, **312-314**, 168 (2002).
29. K. Nakamura and A. Ikawa, *Phys. Rev.*, **B 66**, 24306(2002).
30. X. Y. Liu, M. S. Mo, J. H. Zeng and Y. T. Qian, *J. Cryst. Growth*, **259**, 144 (2003).

Arûnas Jagminas, Indrë Gailiûtë, Gediminas Niaura, Raimondas Giraitis

KONTROLIUOJAMO DYDÞIO GRYNØ Se NANOKRISTALØ SINTEZË PANAUDOJANT AKYTÀSIAS MATRICAS

S a n t r a u k a

Parodyta, kad á aliuminio akytøjø anodiniø oksidiniø matricø (AOM) kapiliarø dugnà nusodinamo kintamàja srove ið vandeniniø selenitinës rûgðties tirpalø amorfinio seleno (a-Se) nanodaleliø dydá (aukðtis iki 100 nm, skersmuo, ¨, nuo 10 iki 70 nm) daugiausia lemia AOM kapiliarø ¨ ir elektrolito temperatûra. Ðvieþiai nusodinto seleno amorfinë bûsena AOM kapiliaruose patvirtinta FT-Raman ir rentgeno difrakciniais spektrais. a-Se sudëtyje aptikta trigonalinio (t-Se) bei Se_8 þiedø priemaiðø. Nustatyta, kad terminio AOM su a-Se uþpilda rekristalizavimo argono atmosferoje metu (T = 438 K) a-Se virsta gryna kristalinio t-Se faze.